



---

*Research article*

# **Denoising deep brain stimulation pacemaker signals with novel polymer-based nanocomposites: Porous biomaterials for sound absorption**

**Baraa Chasib Mezher AL Kasar<sup>1,2</sup>, Shahab Khameneh Asl<sup>1,2,\*</sup>, Hamed Asgharzadeh<sup>1,2</sup> and Seyed Jamaledin Peighambardoust<sup>3</sup>**

- <sup>1</sup> Department of Materials Engineering, Faculty of Mechanical Engineering, University of Tabriz, Tabriz 51666-14766, Iran
- <sup>2</sup> Nanostructured and Novel Materials Laboratory (NNML), Department of Materials Engineering, University of Tabriz, 51666-16471, Tabriz, Iran
- <sup>3</sup> Faculty of Chemical and Petroleum Engineering, University of Tabriz, Tabriz 5166616471, Iran

\* **Correspondence:** Email: sh.kh.asl@tabrizu.ac.ir; Tel: +41-33392468.

**Abstract:** Deep brain stimulation (DBS) pacemakers are sophisticated medical devices that deliver electrical signals to targeted areas of the brain via implanted electrodes, effectively regulating abnormal brain activity and relieving symptoms of treatment-resistant neurological disorders. However, proximity to other electromagnetic equipment may introduce additional noise, which can be disruptive to individuals. To mitigate this issue, we propose a novel polymer-based nanocomposite for pacemakers for signal denoising. This research focused on the development and analysis of nanocomposites comprising polypropylene (PP) combined with montmorillonite nanoclay and graphene nanosheets (GNs). The nanocomposites were created by blending them through melting, using varying ratios of clay to GNs, with a total loading of 4 wt.%. This study focused on enhancing the signal-to-noise ratio for brain pacemakers by using nanocomposites. It investigated the noise reduction properties of PP nanocomposites, specifically in the outlet gate of the pacemaker. This research aimed to find the ideal ratio of clay to GNs in the PP matrix. X-ray diffraction (XRD) and differential scanning calorimetry (DSC) were conducted to analyze the crystalline structure and filler dispersion, as well as thermal behavior and filler–matrix interactions in the material. Scanning electron microscopy was employed to observe the dispersion of the nanofillers in the PP, and sound tube testing was conducted to evaluate the noise levels of the composites. The findings indicated that a porous

structure of the nanocomposite with dispersed microspheres within the PP matrix and a long pathway facilitated increased dissipation of acoustic waves, making it suitable for denoising in brain pacemakers. Furthermore, the nanocomposite containing 2.75 wt.% of nanoclay and 1.25 wt.% of graphene components within the polypropylene matrix demonstrated a favorable signal-to-noise ratio compared to other evaluated nanocomposites.

**Keywords:** deep brain stimulation; polypropylene (PP)/clay/graphene; nanocomposite; denoising properties; porous media

---

## 1. Introduction

Deep brain stimulation (DBS) pacemakers are advanced medical devices that deliver controlled electrical impulses to specific brain regions to treat neurological disorders. Commonly used for conditions like Parkinson's disease, DBS pacemakers aim to improve neural activity, motor function, and symptom relief. However, noise in electrical signals poses a challenge to treatment accuracy and outcomes. Researchers are investigating polymer-based nanocomposites to reduce this noise, potentially enhancing signal clarity and therapeutic benefits for patients with neurological disorders. This innovative approach holds promise for advancing neuromodulation and improving patient care.

Advancements in polymer nanocomposites using nanofillers have improved physical, mechanical, thermal, electrical, and gas barrier properties, resulting in lightweight, flexible, and transparent materials similar to nanomaterials [1]. The characteristics of nanofillers impact the properties of these nanocomposites. Studies show that incorporating layered structures like clay montmorillonite (MMT) and graphene (GNs) can enhance fracture toughness. However, there is limited research on the noise-reduction capabilities of these nanocomposites. Nanocomposites show great potential as sound absorbers in sound-related devices when compared to other materials. Using porous materials in various applications is a common method for reducing noise. The reason porous materials are effective in absorbing sound is because of their many interconnected small pores, which allow sound waves to penetrate the material and dissipate energy through heat loss caused by friction between air molecules and the walls of the pores [2,3]. Porous materials are commonly used for sound absorption, and extensive research has been conducted to investigate how these materials absorb sound. The transmission of sound is influenced by the surrounding environment, with sound absorption being influenced by factors such as humidity and temperature [4].

Clay and graphene nanocomposites are well-known for their mechanical performance and unique functionalities, with clay nanoparticles like MMT having diverse applications and distinctive properties, and graphene offering exceptional properties due to its structure [5,6]. These nanomaterials can potentially be utilized as biomaterials within pacemakers, despite being placed away from tissues and cells, as they are biocompatible. In the medical field, pacemakers are essential devices implanted in patients to regulate heartbeats or brain activity through electrical impulses. Recent advancements focus on incorporating polymer nanocomposites into pacemakers to enhance their performance, considering factors such as biocompatibility, mechanical strength, electrical conductivity, thermal stability, and longevity [7].

Efforts are being made to improve the effectiveness, reliability, and lifespan of pacemakers by incorporating nanocomposites, with researchers like Mohammed et al. [7] conducting studies on the

buckling behavior of microcomposite shells in pacemakers to identify durable materials. They have proposed a new material to address the impact of strong electromagnetic forces on pacemaker microcomposite shells, highlighting the influence of thickness stretching and material properties on critical buckling loads. These findings are relevant to micro-electromechanical systems and can aid in selecting materials for durable and efficient pacemaker nanocomposite shells. Graphene, known for its exceptional strength and unique properties, has gained significant attention since its discovery. It is a promising material for technological applications, especially in polymer nanocomposites, offering flexibility and exceptional mechanical, thermal, electrical, optical, and chemical properties. The performance of graphene-based polymer nanocomposites depends on processing conditions and the even distribution of graphene within the matrix. Achieving this uniform dispersion is challenging and often requires chemical modifications for better dispersibility and bonding. Various manufacturing techniques are used, but questions remain about the role of interfaces in nanocomposites with layered fillers like clay and graphene.

Lee et al. [8] conducted a study on the enhancement of moisture absorption resistance in polypropylene (PP) nanocomposites through the incorporation of hydrophobicity-modified graphene/montmorillonite (MMT-G). This nanocomposite, combining PP with a graphene/montmorillonite hybrid, exhibits waterproofing properties that make it particularly well-suited for pacemaker applications. The study showed a notable enhancement in the water contact angle of MMT-G by 676%. Moreover, the PP/MMT-G nanocomposites exhibited a decrease of up to 11.22% in maximum moisture absorption compared to standard PP composites. As pacemakers are implanted internally, it is essential for them to have resistance to fluids such as blood, cellular secretions, and tissues. Nanocomposites, categorized as biomaterials, are biocompatible even though they do not come into direct contact with cells, tissues, or blood. They demonstrate minimal moisture absorption and efficient thermal conductivity. Wang and colleagues [9] devised a signal-denoising framework for electrocardiograms, leading to a significant enhancement in signal-to-noise ratio (SNR) and diagnostic model accuracy. Similarly, Zhong et al. [10] introduced an innovative approach to evaluate signal quality during the detection of multi-channel fetal electrocardiogram complexes. The accuracy of the detection results is used to estimate the signal quality of each channel. Wen et al. [11] explored intelligent personalized diagnosis modeling in an advanced medical system for Parkinson's disease utilizing voice signals. The focus of the study was on reducing noise in these signals, particularly in the lower range. In essence, for medical devices that come into direct contact with vital human areas such as the heart, blood vessels [12], and brain, designers must carefully choose suitable biomaterials to reduce noise around the equipment.

Saurav et al. [13] explored polymer-based nanocomposites for bone tissue engineering, focusing on natural biopolymers and their blends with other polymers such as cellulose, chitin, chitosan, polylactic acid (PLA), polyhydroxybutyrate (PHB), and silk fibroin. They discussed the structure, preparation, and applications of these blends in tissue engineering. Sagadevan and colleagues [14] discussed the progress made in polymer matrix nanocomposites for bone tissue engineering, highlighting their properties such as bio-inertness, biocompatibility, osseointegration, and their ability to replicate bones, joints, and teeth for orthopedic purposes. Abbas and team [15] explored the latest advancements in polymer nanocomposites for bone regeneration, focusing on the use of nanocomposite scaffolds, ceramics, and biomaterials for the regeneration of bone tissue. They also examined the potential industrial uses of polymer nanocomposites in aiding individuals with bone deficiencies.

Heart pacemakers regulate the heart rhythm with electrical impulses, while brain pacemakers stimulate specific brain regions for movement and neuropsychiatric disorders [16,17]. Our study emphasizes the significance of reducing noise in brain pacemakers to improve signal clarity and patient outcomes. We propose the use of advanced nanocomposites to decrease noise levels and enhance the effectiveness of pacemakers. While previous research focused on mechanical attributes, we are exploring noise-reducing nanocomposites incorporating graphene nanoplatelets and montmorillonite nanoclay. These enhancements are intended to improve the signal-to-noise ratio, thereby optimizing the functionality of brain pacemakers for a range of health conditions. The structure of our investigation is outlined in Figure 1. Initially, we defined our research objectives, recognizing the need for durable and noise-resistant materials in pacemakers where current selection is lacking. Subsequent steps involved developing and creating nanobiocomposites, followed by testing to gain a more complete understanding of material behaviors. In our latest work, we also performed X-ray diffraction testing to analyze the crystal structure and phase composition of nanocomposites at a nanoscale level. This testing aids in determining the atom arrangement, crystalline properties, crystal size, lattice parameters, and orientation of crystalline phases within the nanocomposites, offering valuable insights into their structural features and interactions to optimize properties for specific applications.

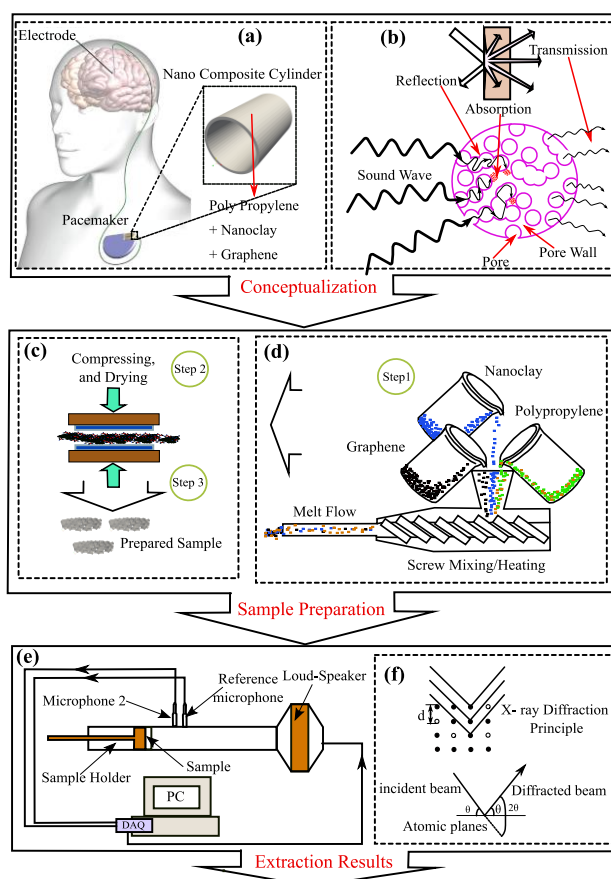


**Figure 1.** Overview of the current study, showing (a) the design of a deep brain stimulation device using innovative biomaterial, (b) the principle of sound wave suppression, (c,d) the preparation process of a nanocomposite, (e) testing of sound tubes, and (f) X-ray diffraction testing.

## 2. Materials and methods

### 2.1. Materials

In the current study, the polymer matrix utilized was polypropylene PP5032 sourced from ExxonMobil Chemicals, renowned for its extrusion/co-extrusion-grade characteristics. This polypropylene variant boasts a melt flow index of 3.0 g/10 min, a density of 0.95 g/cm<sup>3</sup>, and a Vicat softening temperature of 156 °C. The MMT clay employed in the research was procured from Southern Iran, specifically Dasht-Arjan (Shiraz city), and underwent in-house purification processes for nanocomposite production. Additionally, natural flake graphite, sulfuric acid, and formic acid sourced from Asbury Carbons were key components utilized in the experimental procedures.

Uppu et al. [18] investigated the reduction of microcracks in polyurea by incorporating graphene and nanoclay to potentially enhance barrier properties. Analysis of surface images before and after exposure to cryogenic temperatures revealed that the controlled addition of graphene and nanoclay to polyurea thin films can mitigate microcracking from thermal shocks. Safie and Azam [19] successfully produced reduced graphene oxide (rGO) with nanoplatelet morphology using an eco-friendly solution-based method. The resulting rGO displayed a larger crystallite size along the a-axis compared to the c-axis, indicating a nanoplatelet structure, which was further confirmed by morphology analysis.

### 2.2. Clay montmorillonite and graphene preparation

Montmorillonite, or bentonite, is an aluminum silicate mineral prized for its unique properties such as high surface area, swelling capacity, adsorption ability, and mechanical strength. These characteristics make it a valuable resource in various industries like pharmaceuticals, cosmetics, and construction. While raw montmorillonite finds use in applications like drilling mud and ceramics, purified montmorillonite is preferred in pharmaceuticals and cosmetics for its detoxification and cleansing attributes. The separation of montmorillonite from impurities is crucial for maintaining its effectiveness, driving research into purification techniques [20].

Leaching, a process that involves dissolving substances from a solid into a liquid, plays a key role in the chemical purification of clay. This method includes breaking down carbonates, dissolving hydroxides, oxidizing organic materials, and dissolving silica. Carbonated minerals such as calcite can be removed from clay by treating it with mild hydrochloric acid or acetic acid. Acid treatment helps expose crystal edges, making cations soluble and enhancing the clay's adsorption capacity. Iron, aluminum, and manganese (hydr)oxides can be eliminated by forming complexes with citrate. Various chemical combinations are explored for dissolving iron hydroxides, followed by washing with a sodium chloride solution. Organic substances can be eradicated using hydrogen peroxide, sodium hypochlorite, or other oxidizing agents. Lastly, amorphous silica can be dissolved by immersing it in a hot sodium carbonate solution [21]. In the treatment of montmorillonite clay, a suspension was prepared by mixing 10 g of clay with 500 mL of deionized water in a 1 L beaker for 24 h. The resulting solids were washed and centrifuged to obtain particles smaller than 15 mm.

The preparation of graphene oxide nanosheets from multi-layer flakes involved a detailed procedure following the modified Hummer's method. Initially, a controlled process was employed where H<sub>2</sub>SO<sub>4</sub> and KMnO<sub>4</sub> were added to graphite powder under specific conditions to synthesize graphite oxide. This synthesis process included careful temperature control and gradual addition of

reagents to ensure the formation of high-quality graphite oxide [22]. The resulting solution underwent filtration, washing, and drying steps to obtain the desired graphite oxide product. Following the successful synthesis of graphite oxide, the material was further processed by mixing it with deionized water and subjecting it to sonication, centrifugation, and drying processes to produce graphene oxide nanosheets. The sonication step played a crucial role in dispersing the graphene oxide nanosheets in the solution, resulting in uniform dispersion with a concentration of 2 g/mL. Subsequent reduction processes were then applied to the graphene oxide to yield-GNs, which possess unique properties and find applications in various fields such as electronics, energy storage, and materials science.

### 2.3. Nanocomposites preparation

Nanocomposites were created by blending different proportions of clay (MMT) and GNs with PP in a heated internal mixer. The blending process took place at 200 °C and 60 rpm to ensure an even distribution of the fillers within the PP matrix. The procedure began by adding the PP matrix first, then incorporating the clay (MMT) and/or GNs, and mixing for 5 min until a consistent torque was achieved. The resulting nanocomposite was removed from the heated chamber, cut into small pieces, and subjected to hot press molding. Compression molding was carried out using an automatic CARVER press with specific settings: a 100 mm × 3100 mm × 1.5 mm steel mold, both plates heated to 200 °C, and a force of 2000 lbs applied. Subsequently, the nanocomposites were cooled to room temperature using a combination of air and water cooling. Finally, 3D printing was employed to refine the shape of the samples for testing in sound tube devices.

**Table 1.** Composition of the studied formulation (wt.%).

| Cases | Ratio      | Polypropylene | Clay | Graphene |
|-------|------------|---------------|------|----------|
| (a)   | 4: 0       | 96            | 4    | 0        |
| (b)   | 2.75: 1.25 | 96            | 2.75 | 1.25     |
| (c)   | 2: 2       | 96            | 2    | 2        |
| (d)   | 1.25: 2.75 | 96            | 1.25 | 2.75     |
| (e)   | 0: 4       | 96            | 0    | 4        |

The composition of the studied formulation by weight percentage is presented in Table 1. Nanocomposite (a) does not contain graphene components but includes clay and PP. The immiscibility of PP and clay, stemming from their differing polarities, necessitates modifying the clay's polarity to organophilic for effective composite formation. The incorporation of maleic anhydride polypropylene as a compatibilizer can enhance the dispersion of clay within PP. In the montmorillonite clay treatment process, maleic anhydride polypropylene was introduced into the clay particles to alter the clay's polarity to organophilic.

Melt intercalation is the main method to obtain nanocomposites, and normally a twin-screw extrusion is used. The success of the exfoliation by melt blending is associated with the presence of strong interactions between the clay and the polymer chain as well as the diffusion of the polymeric chains into the clay layers. The process efficiency also depends on the temperature, residence time, and screw shear profile. The use of intermediary residence time, low process temperature, and medium shear rates were the best conditions to obtain the dispersion of the clay in exfoliated and intercalated structures.

The significant surface-to-volume ratio of nanoparticles leads to notable enhancements in various properties, such as mechanical characteristics (e.g., tensile strength, stiffness, and toughness), barrier properties, heat resistance, flame retardancy, chemical resistance, and dimensional stability. Silicon- and carbon-based composites are effectively employed in the production of anodes for lithium-ion batteries. The reduced permeation of solvents through polymers is advantageous for applications in components like fuel tanks and fuel lines. Overcoming challenges related to optical issues and dispersion problems associated with nanofillers is essential for maximizing the potential of these materials. The incorporation of graphene components into PP/clay nanocomposites can improve electrical and thermal conductivity, making them suitable for use as noise-reducing agents in nanocomposites [23]. In scenario (e), the nanocomposites exclusively consist of graphene. Graphene-reinforced polymer nanocomposites exhibit superior properties, including high tensile strength, Young's modulus, thermal conductivity, and thermal stability. Patra and colleagues [24] employed the thermoplastic polymer "polypropylene" through melt mixing to develop nanocomposites with graphene, utilizing various experimental methods to thoroughly analyze the physicochemical properties of the nanocomposite. The experimental findings suggest that both the content and size of graphene have specific positive and negative effects on filled polypropylene composites. Generally, increasing the graphene content in polypropylene yields favorable results. In our study, the use of 5  $\mu\text{m}$  GNP sheets proved beneficial in most instances, although sheets sized at 15  $\mu\text{m}$  performed better in terms of flexural and impact strength.

#### 2.4. Sound tube testing

Assessing the acoustic properties of polymer nanocomposites is crucial for various applications. Due to proposing the nanocomposites as outlet gates of brain simulator pacemakers, we investigated the acoustic properties of five mentioned nanocomposites. The focus of the research was on investigating the sound transmission loss (STL) property. The denoising properties of a composite were assessed using STL method, which is defined as the difference between the incident and transmitted sound power levels. The STL intensity in decibels (dB) is given by the Eq 1 [25]:

$$STL(dB) = 10 \log\left(\frac{I_i}{I_t}\right) \quad (1)$$

$I_i$  represents the incident acoustic power, and  $I_t$  refers to the transmitted acoustic power. They are defined as follows [25]:

$$I_t = \frac{1}{2} \operatorname{Re} \iint_A P_t V_t^* dA \quad (2)$$

$$I_i = \frac{1}{2} \operatorname{Re} \iint_A P_i V_i^* dA \quad (3)$$

where \* and Re denote the conjugate complex number and the real part, respectively.  $V_i$  and  $V_t$  are the fluid particle velocity in the incident and transmitted domains, respectively [25]. The research involved

measuring both incident and transmitted acoustic power using the impedance tube method, employing equipment such as microphones, an impedance tube, a conditioning amplifier, a frequency analyzer, and software at room temperature. STL values were determined for nanocomposites containing fillers like graphene and nanoclay. The impedance tube setup consists of a long cylindrical tube with microphones positioned at each end, separated by the test sample. Sound waves travel through the sample, and the microphones record sound pressure levels before and after, facilitating the calculation of STL. This setup allows for the evaluation of materials' acoustic properties for sound blocking or absorption, aiding researchers in assessing their efficacy in reducing sound transmission, which is vital for optimizing material design for specific applications. It is worth noting that the sample must have a 35 mm diameter to fit in the impedance tube. The tube utilized a microperforated panel (MPP) with 50 and 100 mm air cavities and a sinusoidal signal as the excitation source. The study demonstrated that the transfer-function method for measuring sound absorption coefficients in small samples is both simple and accurate. Nanocomposites, with their porous structure and ability to absorb sound waves, are ideal for soundproofing applications. The addition of nanoparticles further enhances their sound absorption capabilities by increasing surface area and altering the material's structure at a molecular level. Ultimately, nanocomposites have the potential to revolutionize the field of soundproofing materials.

### 2.5. Electrophysiology probe for signal-to-noise ratio calculations

The electrophysiology probe station, a specialized lab equipment for studying the electrical activity of biological cells or tissues, utilizes microelectrodes for stimulation and recording, amplifiers for signal enhancement, a stimulus generator, temperature control, and data analysis software. Researchers employ these stations to investigate neurons, cardiac cells, and other tissues, exploring action potentials, ion channels, and synaptic transmission to understand physiological processes and pathologies. To assess the samples' SNR, a custom-built probe station maintained at 20 °C was used, with a multi-clamp 700B amplifier applying sinusoidal voltage signals to nanocomposite materials for precise SNR measurements under controlled conditions [26]. The voltage signal response was measured with respect to the grounded external contact by a probe connected to an oscilloscope. All the measurements were performed at room temperature. Finally, a conversion of voltage to current was done based on the head stage circuit, which is a non-inverting amplifier with a feedback resistor equal to 500 MW. The gain of this amplifier is calculated as shown in Eq 4. In electrophysiology, a voltage clamp involves applying a voltage (input) and observing the current response (output). The voltage clamp gain is calculated in Eq 4 [26].

$$Gain = \frac{V_{out}}{I_{in}} = \frac{0.5 \text{ V}}{1nA} = 0.5V / nA \quad (4)$$

SNR is calculated by comparing the measured signal to the average baseline noise. This involves performing a Fourier transform of the current signals over time and analyzing the frequency spectrums.



## 2.6. Scanning electron microscopy (SEM) measurements

The SUPRA 55 FESEM/EDX system from Carl Zeiss, Germany, was utilized to analyze the morphology in detail. Operating at 30 kV, the electron gun provided the necessary energy for imaging. The system boasted an impressive instrumental resolution of 1.4 nm at 15 kV, allowing for high-quality imaging and precise analysis of the sample's structure and composition. This advanced equipment enabled researchers to obtain accurate and detailed information about the sample's morphology, aiding in a comprehensive understanding of its characteristics.

In practical contexts, as structures undergo aging, alterations in their material attributes and stress levels are induced by shifts in environmental circumstances and the duration of operation [27]. Vital steps to combat these changes encompass regular upkeep, comprehensive evaluations, and the application of predictive modeling. By overseeing the structural state, pinpointing degradation catalysts, and promptly rectifying issues through maintenance, the adverse effects of aging can be mitigated. Moreover, considering the ambient environmental conditions and enacting protective measures can assist in upholding the structural durability over an extended operational lifespan [28]. The crystallization process in polymers is intricate, influenced by variables like temperature, cooling speed, and nanoparticle traits. Ensuring efficient control of crystallinity in composite polymeric systems is pivotal for enhancing material characteristics, yet conflicting research results on the impact of nano-additives pose hurdles in achieving empirical regulation.

## 2.7. X-ray diffraction

The X-ray diffraction (XRD) analysis was conducted using a Siemens D500 instrument with Cu ( $\lambda = 1.54 \text{ \AA}$ ) to investigate the basal spacing of nanoclays, graphene, and the structure of nanocomposites. The basal spacing of the clays was determined by analyzing the (001) peak in the XRD pattern using the Bragg equation  $\lambda = 2d \sin\theta$ , where  $\lambda$  represents the wavelength. Crystalline materials exhibit a regular atomic arrangement. When exposed to X-rays of specific wavelengths, the electrons within the material interact with the radiation through elastic collisions, causing them to oscillate. This results in the creation of a coherent source of electromagnetic radiation at the same frequency and phase as the incoming X-rays. The emitted radiation from various atoms may either undergo constructive or destructive interference. By measuring and analyzing the diffraction peaks resulting from constructive interference, the desired crystal properties can be calculated.

## 2.8. Crystallization (Crys) and melting temperature

For the examination of thermal properties, specifically the crystallization and melting temperature of the PP-based material, differential scanning calorimetry (DSC) tests were conducted using a PerkinElmer DSC 8500 instrument. Approximately 15 mg of the sample underwent temperature cycling from  $-25$  to  $180 \text{ }^\circ\text{C}$  under a nitrogen atmosphere. The samples were heated and cooled at a rate of  $10 \text{ }^\circ\text{C}/\text{min}$  in three consecutive scans: heating, cooling, and heating. Three separate runs were performed for each sample. The initial heating scan served to eliminate the sample's thermal history, the cooling scan identified the crystallization temperature ( $T_c$ ), and the second heating scan determined the melting temperature ( $T_m$ ) along with the melting enthalpy ( $\Delta H_m$ ).

### 3. Results

#### 3.1. SEM analysis

The SUPRA 55 FESEM/EDX equipment was used to examine the microstructures of the materials, allowing for the assessment of how effectively the clay and graphene components were dispersed within the polymeric materials. Prior to the SEM analysis, the materials were mixed at 200 °C to reach the necessary viscosity for mixing while minimizing degradation, with a rotation speed of 60 rpm. Following the addition of all components into the mixer, melt mixing was extended for an extra 5 min for each 40 g batch to ensure a suitable volume for the mixer. The total concentration of nanoclay and graphene in all nanocomposite samples was consistently maintained at 4 wt.%. Subsequently, the sample surfaces were polished and coated with gold. The use of scanning electron microscopy (SEM) provided valuable insights into the dispersion and distribution of clay and GNs within the PP matrix. The SEM images in Figure 2 demonstrate a uniform dispersion of clay and GNs in the PP matrix without observable filler clusters, even in case (e). This suggests that the melt-compounding conditions used were ideal for producing these nanocomposites, indicating potential benefits for customized composite properties suitable for noise reduction applications. The research also investigated the potential applications of these nanocomposites in brain pacemakers, as illustrated in Figure 2a,b, displaying intricate pore structures intertwined with fibers. The images highlight the formation of pores caused by solidified adhesive influenced by the polypropylene agent, emphasizing the pore formation in the composite due to gaps between fibers and those induced by the polypropylene agent.

Moreover, the research illuminated the influence of nanocomposite density on sound insulation properties, with the denser sample (case b) exhibiting the highest STL values attributed to its irregular hole structures and increased density. Additionally, the study observed a trend where increasing graphene percentages led to a decrease in nanocomposite density, consequently resulting in diminished STL values. Furthermore, the specific dimensions of the hollow polypropylene spheres depicted in Figure 2a,b, including inner and outer diameters and shell thickness measurements, were detailed. The research primarily focused on the design of ternary polypropylene, nanoclay, and graphene nanocomposites, with sound insulation tests showcasing excellent performance, particularly in the case of composite (b) containing 2.75 wt.% nanoclay and 1.25 wt.% graphene. The presence of nanoclay particles was identified as a key factor in enhancing the denoising capabilities of the nanocomposites, with case (b) exhibiting promising results for sound absorption applications in pacemaker shells compared to case (e) with 4 wt.% graphene. This comprehensive investigation sheds light on the potential advancements in denoising technology and offers valuable insights for future research in this domain.

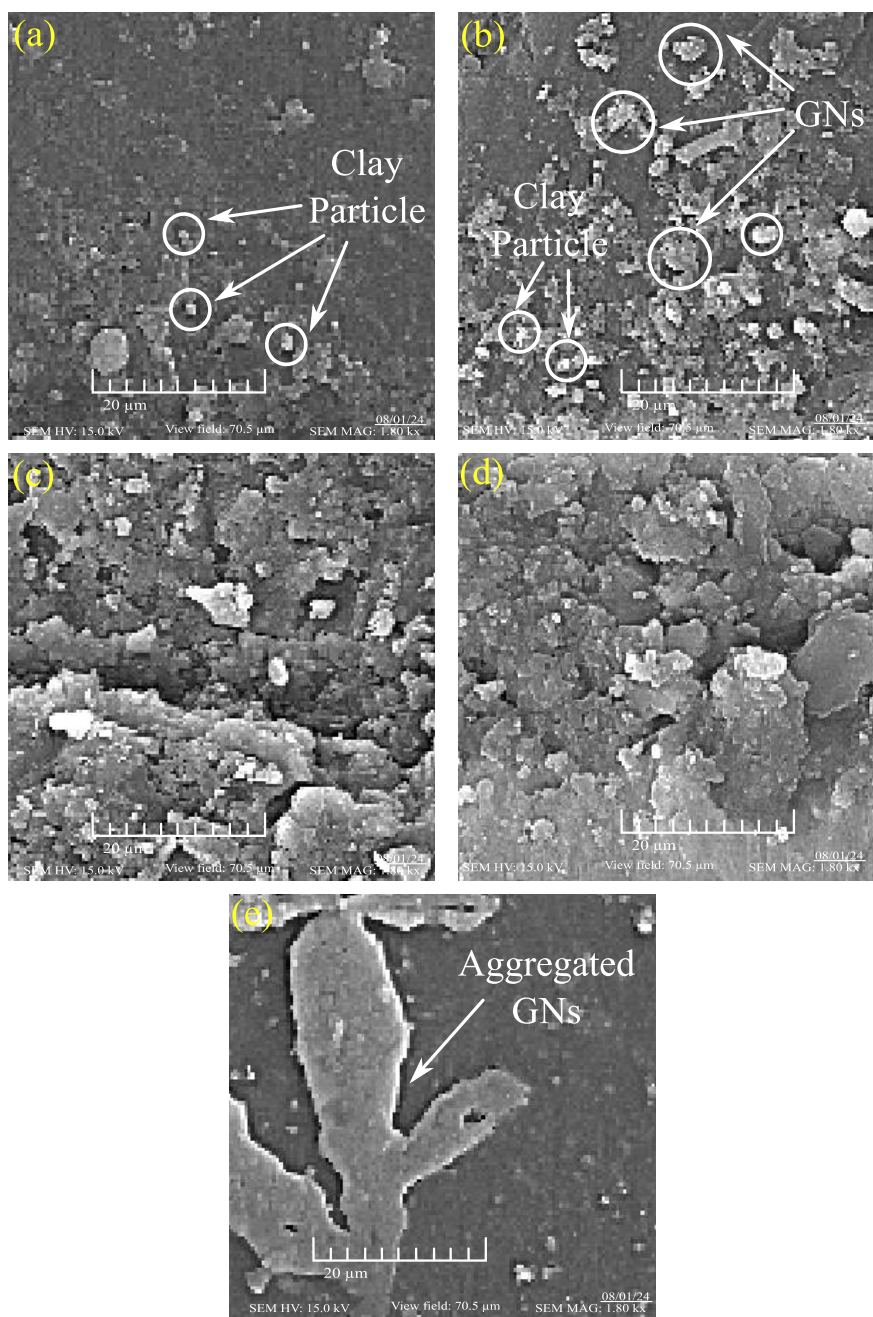


**Figure 2.** SEM images of different nanocomposites. (a): PP/4%Clay/0%GNs, (b): PP/2.75%Clay/1.25%GNs, (c): PP/2%Clay/2%GNs, (d): PP/1.25%Clay/2.75%GNs, (e): PP/0%Clay/4%GNs.

### 3.2. Noise calculations

The field of denoising materials is crucial for creating environments that are conducive to concentration, relaxation, and overall well-being. A higher STL value is indicative of superior denoising capabilities, which is essential in various settings such as residential, commercial, and industrial spaces. The combination of PP/graphene/clay in composites has garnered attention due to

their promising mechanical and thermal properties. These composites have shown versatility and applicability across a range of industries, from construction to electronics. This study delves specifically into the sound barrier properties of PP/graphene/clay composites, aiming to enhance our understanding of their effectiveness in reducing noise transmission. The findings suggest that a higher clay percentage in the composites leads to improved denoising performance compared to those with just graphene or clay particles, especially across different frequencies. Figure 3a provides a visual representation of the denoising performance of the nanocomposite of PP/graphene/clay, offering insights into how these materials behave under varying frequency ranges. The specific composition of PP/2.75%Clay/1.25%GNs stands out for its unique characteristics, such as small microspheres and long cavities, which contribute to enhancing the denoising properties of the nanocomposites when utilized inside pacemaker shells. Noise within pacemakers can pose significant challenges for individuals relying on these devices, disrupting their daily activities and overall quality of life. As a result, research efforts have been directed toward developing sound-insulating and absorbing materials to mitigate this issue across a wide range of applications. The intersection of material science and neurotechnology in this study represents a novel approach to addressing the need for improved materials in the field of neuroscience. By leveraging the properties of micro shells and innovative electrode designs, this research aims to advance the development of cutting-edge technologies that can enhance the performance and longevity of medical devices like pacemakers.

Sound insulation involves the rapid elevation of STL curves [29]. The dip in sound insulation occurs when the frequency of the incoming wave matches the natural frequency of nanocomposites. Essentially, when the structure resonates, it results in an increase in the sound power transmitted. It is observed that the dip in sound insulation of PP/2.75%Clay/1.25%GNs shifts to higher frequencies when compared to PP/0%Clay/4%GNs and PP/4%Clay/0%GNs. In simpler terms, incorporating both fillers into the polymer matrix is crucial for creating an effective nanocomposite for brain pacemakers.

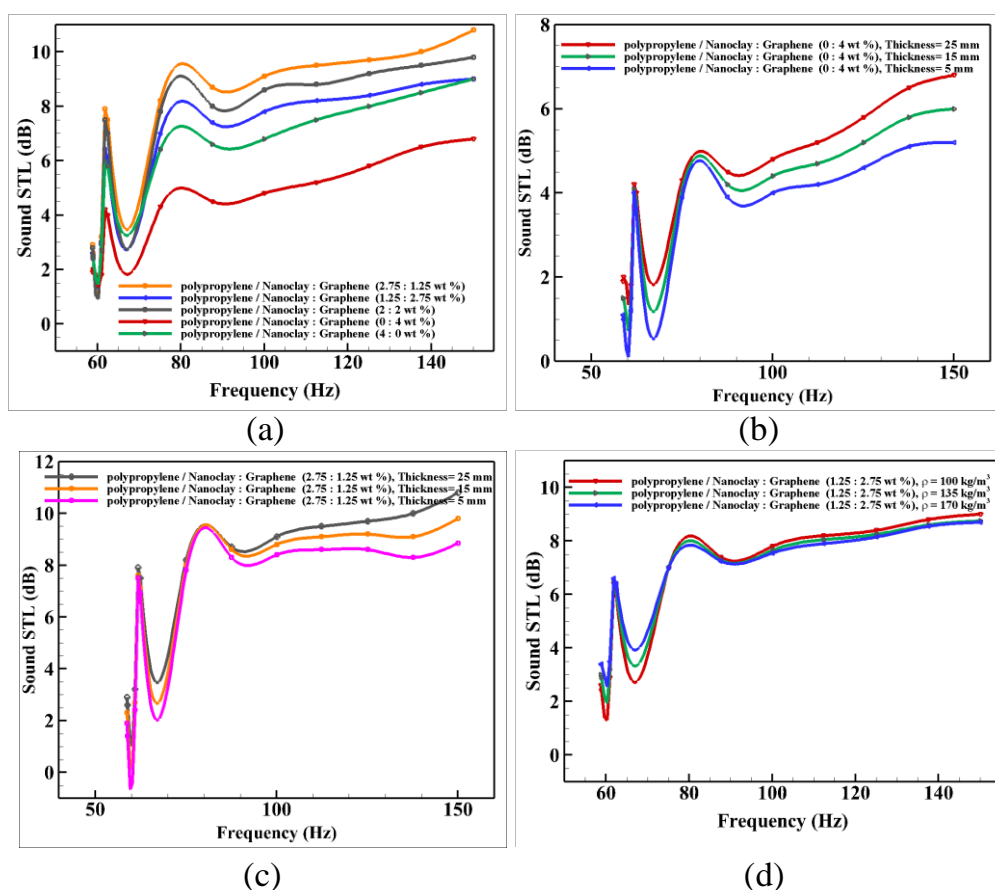


**Figure 3.** (a): STL of nanocomposite of PP/graphene/clay (55–150 Hz), (b) and (c): effects of various sample thicknesses on STL of nanocomposites, (d): effects of density.

In the context of pacemakers, there is an overlap between the electromagnetic radiation (0–60 Hz) and cardiac signal frequency ranges, which can affect the pacemaker's functionality if filtered out using bandpass filters. European standards mandate that pacemakers must withstand electromagnetic interference up to a specific voltage level determined by frequency. Healthcare professionals working with pacemaker patients need to be vigilant in monitoring and addressing potential issues related to electromagnetic interference, adjusting sensitivity settings to avoid detecting interference below the recommended voltage threshold. Our research focusing on sensitivity settings and 50 Hz noise thresholds in a large population can aid healthcare providers in programming settings to prioritize patient safety in the presence of electromagnetic interference. STL was assessed by evaluating intensity changes within the 0–150 Hz frequency range, with findings indicating that nanocomposites performed well near the 50 Hz noise thresholds.

### 3.3. Effects of sample thickness on STL

In addition to examining the impact of sample thickness on the STL of nanocomposites, the study also delves into the relationship between bulk density and sound absorption. The nanocomposites under investigation include PP/2.75%Clay/1.25%GNs and PP/0%Clay/4%GNs, with a consistent bulk density of  $100 \text{ kg/m}^3$  maintained for all samples. Figure 3b,c visually represent the observed increase

in sound absorption with greater sample thickness, resulting in a wider absorption bandwidth, particularly noticeable at lower frequencies.

Samples were created with different fiber weights while keeping the material volume constant to study how bulk density impacts sound absorption. The results show that sound absorption increased with higher density, supported by SEM images in Figure 2 displaying density distributions. Higher bulk density had a more significant effect on sound absorption across frequencies compared to sample thickness. Greater densities led to increased energy dissipation within the absorber due to enhanced sound path complexity, as shown in Figure 3d. This highlights the vital role of bulk density in improving sound absorption in nanocomposites.

Glé et al. [30] investigated the sound-absorbing properties of hemp fiber and concrete, noting the impact of excess water content on sound absorption coefficients between surfaces [31]. Additionally, Pan et al. [32] explored the potential of discarded carpets as sound-absorbing materials, using compression molding with PP as the matrix material. Their research indicated that compression-molded PP carpets and other carpet composites exhibited superior sound absorption compared to jute/PP composites. Other research efforts, such as studies on high-temperature nanocomposites for microwave absorption applications [33] and FDM filaments incorporating natural fiber-reinforced biocomposites [34], have contributed to expanding knowledge on nanobiocomposites. The present study focuses on novel biomaterials for denoising inside pacemakers.

#### 3.4. XRD and differential scanning calorimetry

The X-ray diffraction patterns in Figure 4a,b demonstrate the characteristic peak of the 001 plane and interlayer spacings of the clay and graphene. The peak of nanoclay and polypropylene without graphene is seen at  $2.42^\circ$ , indicating an interlayer distance of 3.41 nm. In the nanocomposites PP/2.75%Clay/1.25%GNs and PP/0.0%Clay/0.0%GNs, peaks are observed at  $2.15^\circ$  (3.6 nm) and  $2.0^\circ$  (3.95 nm) respectively, suggesting an increased interlayer distance compared to PP/4.0%Clay/0.0%GNs, showing intercalation of PP between the clay layers. The process of intercalation and exfoliation during the melt state is not fully understood. Some researchers believe that interactions between polar groups, shear forces from extrusion, and molecular diffusion within the clay layers may promote intercalation and exfoliation. Figure 4b supports the intercalation process, indicating an increased interlayer distance with higher graphene content. DSC was used to analyze the crystallization characteristics and melting temperatures of pure PP and its nanocomposites filled with clay and graphene materials. The presence of nanofillers only minimally affected the melting and crystallization temperatures of pure PP. The introduction of nanoparticles slightly lowered the crystallization temperature of pure PP while maintaining a consistent melting point. The crystallization temperature of the PP nanocomposites containing different ratios of clay and graphene nanoparticles decreased to varying degrees compared to pure PP, with melting temperatures remaining stable at  $165^\circ\text{C}$  for both the nanocomposites and pure PP. This decrease in crystallization temperature can be attributed to the unmodified surface of the nanoparticles, which lack nucleating capabilities to enhance crystallization temperature. Surface-modified nanoparticles, on the other hand, exhibit nucleating abilities. The width of the DSC crystallization peak is important, as narrower peaks indicate the nucleating function of the filler, aiding polymer crystallization. The higher crystallinity observed in pure PP compared to the nanocomposites is due to the hindrance caused by the nanoparticles in the regular packing of polymer molecules into a highly crystalline structure. A comparison of the elastic moduli of the PP produced in this study and the PP

studied by Dong and Bhattacharyya [6] is presented in Table 2. The results demonstrate a strong agreement between the findings of this study and their research. The dynamic mechanical properties of the nanocomposites are detailed in Table 3, as shown in Figure 4.

**Table 2.** Comparing elastic modules of produced PP and Dong and Bhattacharyya [6].

| Process of Preparing | Temperature (°C) | Present Work | Dong and Bhattacharyya [6] |
|----------------------|------------------|--------------|----------------------------|
| Melt Mixing          | 15               | 1.508 GPa    | 1.510 GPa                  |
|                      | 30               | 1.204 GPa    | 1.208 GPa                  |
|                      | 45               | 1.00 GPa     | 0.991 GPa                  |
|                      | 60               | 0.750 GPa    | 0.751 GPa                  |

**Table 3.** Dynamic mechanical properties of the nanocomposites according to Figure 4.

| Cases | Ratio (Clay: Graphene) | T <sub>10%</sub> (°C) | T <sub>50%</sub> (°C) | T <sub>m</sub> (°C) | T <sub>c</sub> (°C) |
|-------|------------------------|-----------------------|-----------------------|---------------------|---------------------|
| (a)   | 4: 0                   | 198                   | 221                   | 162                 | 113                 |
| (b)   | 2.75: 1.25             | 190                   | 219                   | 162                 | 114                 |
| (c)   | 2: 2                   | 202                   | 230                   | 164                 | 115                 |
| (d)   | 1.25: 2.75             | 210                   | 240                   | 165                 | 115                 |
| (e)   | 0: 4                   | 230                   | 255                   | 166                 | 115.5               |

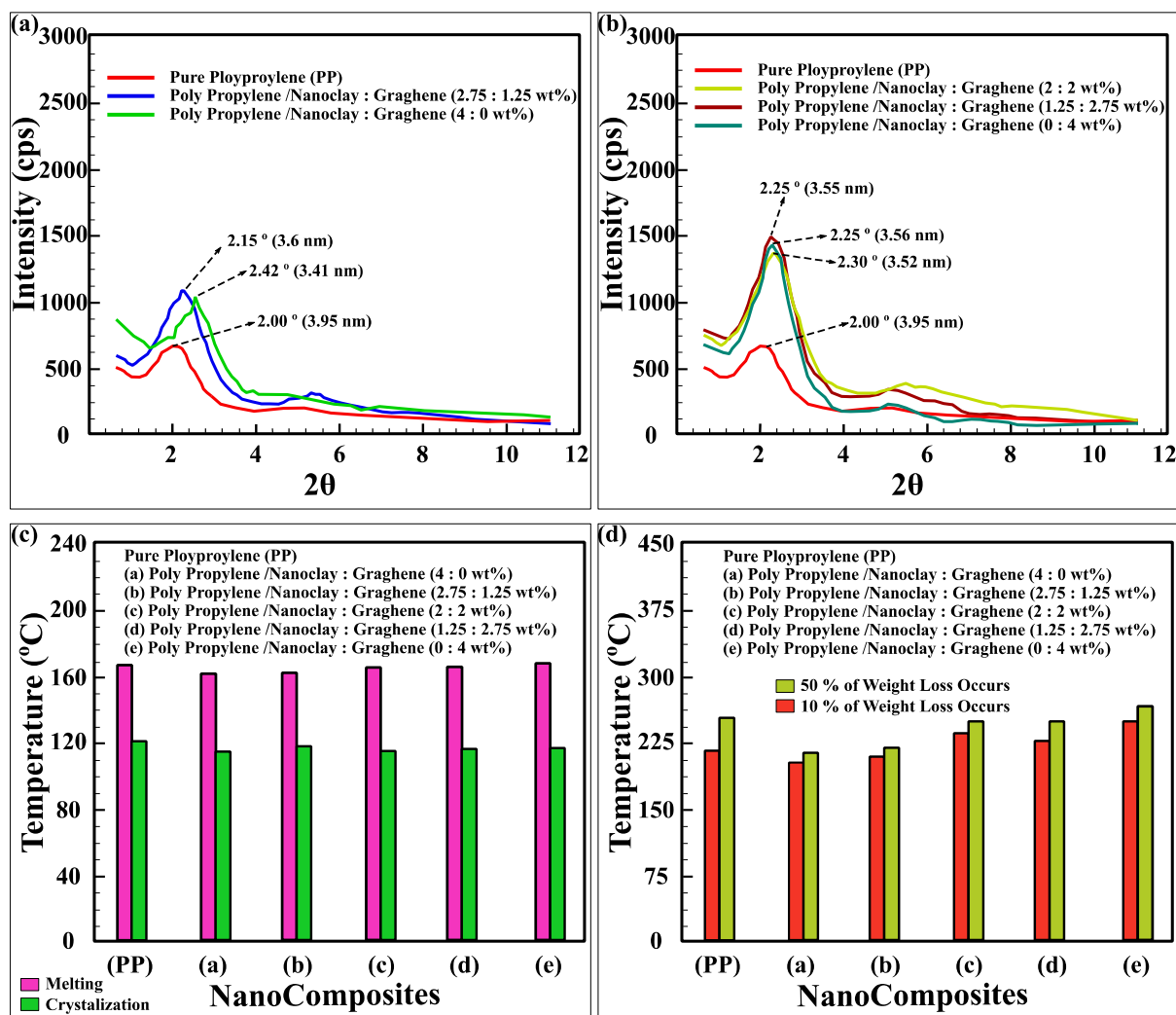


**Figure 4.** (a,b) XRD Patterns of nanocomposites, (c,d) Dynamic mechanical properties of the nanocomposites.

### 3.5. SNR calculations

Initially, baseline noise levels are assessed by introducing a zero-volt signal to the micropipette in solution and recording the current response over time at the external contact. Following this, sinusoidal voltage signals with different frequencies and amplitudes are applied, and the resulting current is measured at the external contact. The frequency spectrums of these current signals over time are subsequently analyzed using the Fast Fourier Transform (FFT) function in MATLAB. Figure 5 illustrates the FFT analysis displaying the current responses for all cases, while Table 4 summarizes the baseline noise measurements for the proposed nanocomposites. Notably, case (b) PP/2.75%Clay/1.25%GNs exhibited reduced baseline noise levels, suggesting its efficacy in noise reduction within pacemaker nanocomposites. Conversely, case (c) PP/2%Clay/2%GNs demonstrated a 78% higher noise level compared to case (b). Increasing graphene content in the composite can improve low-frequency sound absorption by altering the morphology and structure for enhanced acoustic energy dissipation. However, this adjustment may not be optimal for higher frequencies,



potentially leading to acoustic energy amplification. Moreover, our morphology assessment revealed that a higher graphene percentage might lead to the formation of small cavities of limited length, which could impede effective acoustic energy dissipation. While well-dispersed graphene fillers can reduce the average cell size of polypropylene through nucleation, in this study, the average cell size of all nanocomposites, except for case (e), increased compared to the baseline. The increase in denoising properties observed in composites is likely attributed to graphene agglomeration, leading to uneven cell nucleation and the formation of large voids. To overcome this issue, potential solutions include reducing the graphene concentration in the composites or improving graphene dispersion within polypropylene. Acoustic emission and absorption studies on composites can demonstrate their denoising capabilities, showcasing how these materials interact with acoustic waves under different conditions. Satour et al. [35] applied acoustic emission techniques to identify damage in composites, with AE signals indicating compressive failure. In their work, they used a novel algorithm to denoising the signals. Acoustic emission testing involves monitoring sounds during stress application to detect internal flaws, while acoustic absorption refers to a material's capacity to absorb sound energy. This property is critical for noise control, with highly absorptive materials utilized across industries to mitigate noise pollution. In summary, acoustic emission testing offers valuable insights into composite conditions, while acoustic absorption plays a crucial role in noise control and enhancing sound quality. Both aspects are essential in acoustics and materials engineering to ensure structural integrity and acoustic comfort. More researchers tried denoising the signals inside the various materials such as carbon-epoxy-resin composites [36] and graphene oxide–functionalized nanocomposites [37].

Acoustic waves, with their weak damping and longer wavelengths [38], have a distinct diffraction and penetration capability compared to other wave types, making their manipulation more challenging. Research on how acoustic waves propagate, absorb, or reflect in traditional materials has uncovered various issues. For example, these materials struggle to effectively absorb and reflect sound in the low-frequency range, limiting their ability to control low-frequency noise comprehensively. Modern nanocomposites can confine acoustic waves within the pores of structures and dissipate them efficiently. Yang et al. [39] found that sound energy converts to heat energy through internal friction from shear viscosity, with higher dissipated energy corresponding to longer pores in the structure. They introduced Archimedean spiral channel-based acoustic metasurfaces to suppress low-frequency noise effectively at subwavelength levels, aligning with current research. Wen et al. [40] presented an innovative origami-based acoustic metamaterial for dissipating acoustic energy, offering airflow permeability, high design flexibility, and programmability suitable for biomedical applications.

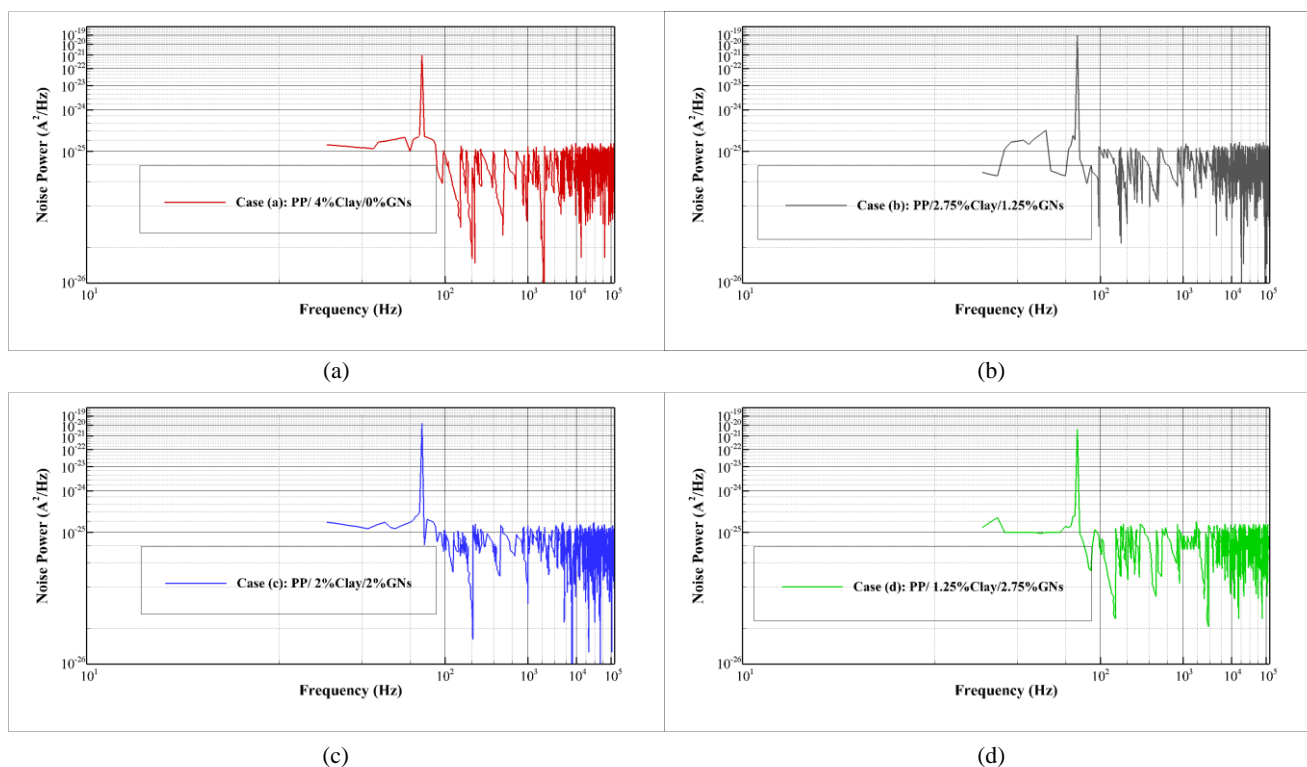


**Figure 5.** FFT of the measured current response to voltage applied for the case (a) PP/ 4%Clay/0%GNs, case (b) PP/2.75%Clay/1.25%GNs, case (c) PP/ 2%Clay/2%GNs, and case (d) PP/ 1.25%Clay/2.75%GNs.

Baseline noise in FFT charts is crucial for accurately detecting noise power levels. It represents the background noise in a signal, impacting the identification of desired signal components. By establishing a baseline noise level, engineers can differentiate between the signal of interest and noise interference, aiding in determining signal-to-noise ratios and data quality evaluation [41]. Accurate noise power detection is vital in applications like telecommunications and audio processing. Monitoring and analyzing baseline noise in FFT charts help to optimize signal processing, filter out unwanted noise, and improve overall signal quality for precise data analysis and interpretation.

Managing noise pollution is essential, and employing sound-absorbing materials is a practical approach to regulating noise levels. These materials are classified into porous and resonant types based on their sound absorption mechanisms. Porous materials feature internal pores that convert sound energy into thermal energy through friction with air molecules, demonstrating effectiveness at high frequencies but less so at low and medium frequencies. Resonant materials, akin to Helmholtz resonators, specialize in absorbing low-frequency sound waves via resonance effects. Nanofibers, with their high specific surface area, excel at absorbing low-frequency sound waves that conventional materials struggle to capture. Utilizing materials like polypropylene, graphene, and nanoclay for producing micro/nanofibers offers increased collision opportunities for sound waves and improved absorption of acoustic energy, presenting a promising avenue for developing advanced sound absorption materials. The study focused on mitigating noise in brain pacemaker medical devices, which can produce disruptive noises when influenced by external electromagnetic or electrical devices. The direct link between the pacemaker and external noisy signals can create discomfort for individuals. Evaluating various polymer-based nanocomposites for these devices was a key objective, given that a

significant majority of pacemakers globally incorporate polymer-based materials. This spurred the exploration of new materials and their testing to enhance comprehension of nanocomposite applications in this specific context.

**Table 4.** Baseline noise measured for proposed nanocomposites.

| Cases | Ratio      | Baseline noise ( $A^2/Hz$ ) |
|-------|------------|-----------------------------|
| (a)   | 4: 0       | $1.81 \times 10^{-26}$      |
| (b)   | 2.75: 1.25 | $0.50 \times 10^{-26}$      |
| (c)   | 2: 2       | $0.89 \times 10^{-26}$      |
| (d)   | 1.25: 2.75 | $1.22 \times 10^{-26}$      |

Figure 6 provides insights into how the SNR of the analyzed nanocomposite varies with the frequency and amplitude of the sinusoidal signal applied. The data clearly shows that the incorporation of nanoclay and graphene enhances the sound absorption characteristics of polypropylene, particularly at lower frequencies. This enhancement holds significant promise for the advancement of sound-absorbing materials tailored for pacemakers. Low-frequency sound waves, known for their elongated wavelength and sluggish speed, pose challenges in terms of attenuation, with prolonged exposure potentially posing health risks.

Emphasizing the prevalence of low-frequency ranges near pacemakers, the study by Kiddell et al. [42] delves into how weak adhesion points within graphene composites can affect their acoustic characteristics. Optimal interfacial adhesion is achieved by covalently attaching graphene flakes to the matrix. In contrast, weaker bonding interactions such as hydrogen bonds and Van der Waals forces can result in inadequate adhesion and load transfer, with these bonds being vulnerable to breaking under minimal stress and reforming once the stress dissipates [43,44]. This cyclic process leads to interfacial sliding between filler particles and the matrix, aiding in sound energy dissipation through friction. The research suggests that robust interfacial adhesion is observed when graphene flakes are covalently linked to polypropylene, reducing interfacial sliding between graphene fillers and the polypropylene matrix. Several studies underscore graphene's importance in polymer-based nanocomposites [45–50]. The introduction of innovative biomaterials could potentially revolutionize the pacemaker industry. Implantable pacemakers are composed of metals, ceramics, glasses, and polymers [51]. The disruption of pacemakers' electrical functions by electromagnetic interference presents a challenge. Our study aimed to improve signal transmission and minimize interference through optimized biomaterials. Healthcare providers should adjust sensitivity settings to effectively manage electromagnetic interference (EMI). European regulations specify voltage endurance levels for pacemakers based on frequency. Our research on sensitivity settings and 50 Hz noise thresholds assists healthcare providers in prioritizing patient safety in the presence of EMI. Additionally, the inclusion of graphene can enhance signal transmissivity, while the incorporation of nanoclay can create pores of suitable size to capture sound waves [52,53].

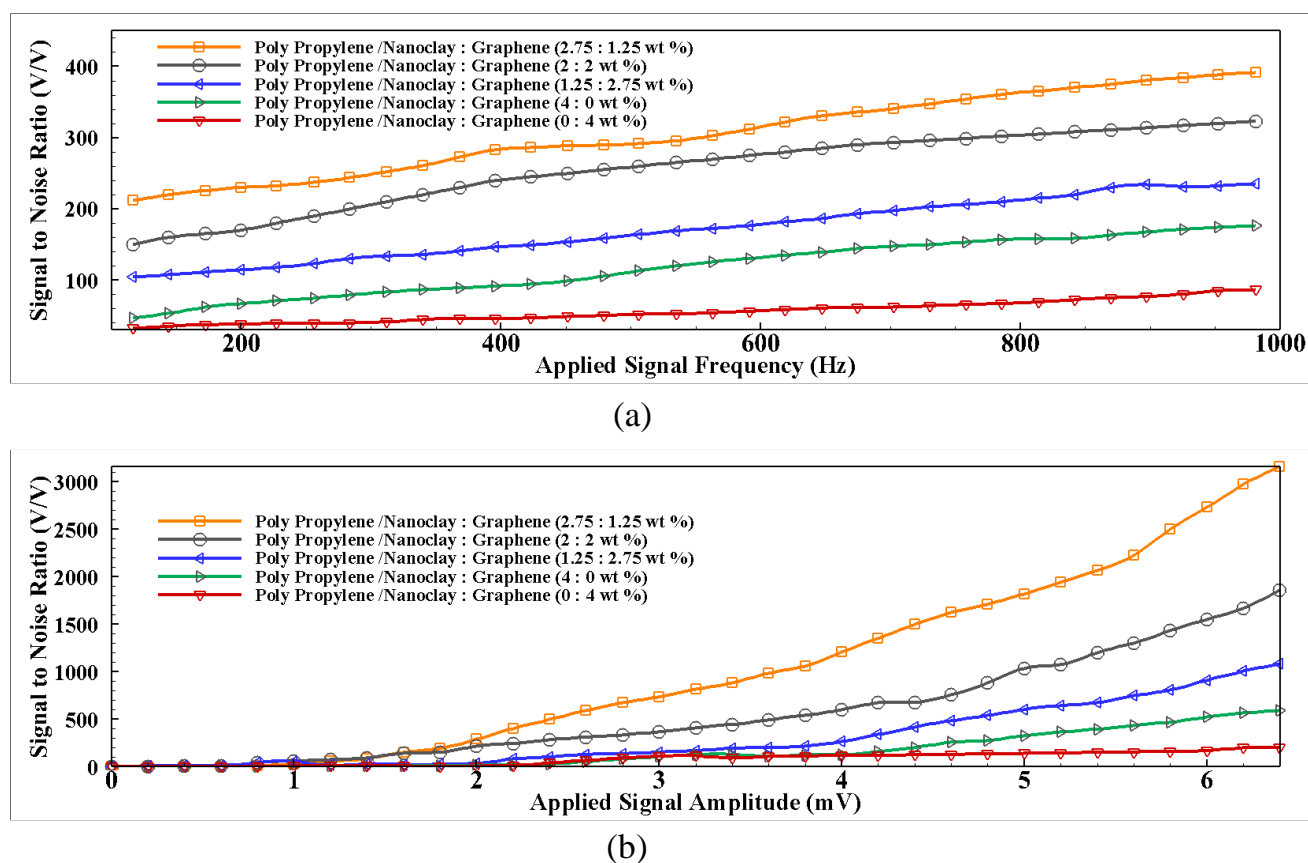


**Figure 6.** SNR of the nanocomposite under study versus the (a) frequency of the applied sinusoidal signal and (b) amplitude. In this figure, signal-to-noise is the ratio of two signals with the unit of V/V.

#### 4. Conclusions

This study aimed to address noise issues in brain pacemaker medical devices, which can be affected by electromagnetic or electrical interference from other devices. Despite advancements in technology to minimize noise in everyday environments, there is still a need for more effective materials. Direct exposure of pacemakers to external noise can cause discomfort for individuals. The research focused on evaluating polymer-based nanocomposites for these medical devices, as the majority of pacemakers globally utilize polymer-based materials. This led to the exploration and testing of new materials to enhance understanding of nanocomposite applications in this specific field.

We also performed X-ray diffraction testing to analyze the crystal structure and phase composition of nanocomposites at a nanoscale level. The research utilized SEM to examine the distribution of clay and GNs within a PP matrix. The SEM images revealed well-dispersed clay and GNs in the PP matrix, indicating favorable conditions for manufacturing these nanocomposites for noise reduction purposes. The study explored the use of these nanocomposites in brain pacemakers, focusing on intricate pore structures and how nanocomposite density affects sound insulation properties. Higher concentrations of clay were found to enhance noise reduction effectiveness, especially across different frequencies.

SNR assessments were conducted to evaluate the noise reduction capabilities of the nanocomposites, with a specific emphasis on PP/2.75%Clay/1.25%GNs for enhancing noise reduction in pacemaker casings. Analysis using FFT showed varied current responses for different nanocomposite compositions, with PP/2.75%Clay/1.25%GNs demonstrating reduced baseline noise levels in case (b). The study also discussed the impact of graphene content on sound absorption and structure, highlighting the importance of well-dispersed graphene in polypropylene for the effective dissipation of acoustic energy.

Overall, this research provides valuable insights into potential advancements in noise reduction technology and the development of sound-absorbing materials tailored for pacemakers. It introduces innovative concepts and materials for sound-insulation studies, offering a promising solution to noise-related challenges in pacemakers.

### **Use of AI tools declaration**

The authors declare they have not used Artificial Intelligence (AI) tools in the creation of this article.

### **Conflicts of interest**

The authors declare no conflict of interest.

### **Author contributions**

All authors equally contributed to the study conception and design, material preparation, data collection and analysis, and writing of the manuscript. All authors read and approved the final manuscript.

### **Acknowledgments**

We appreciate the assistance of the laboratory team in providing the extra data. The X-ray diffraction test and material preparation were carried out at the Nanostructured and Novel Materials Laboratory (NNML) at the University of Tabriz, overseen by Dr. Shahab Khameneh Asl and Dr. Hamed Asgharzadeh. We are thankful for the valuable contributions of the laboratory members during the discussions related to this study. The SEM measurements were conducted at the laboratory of materials at Baghdad University, and Baraa C-M expresses gratitude to the members of this laboratory.

### **References**

1. Manop D, Tanghengjaroen C, Putson C, et al. (2024) The effect of polyaniline composition on the polyurethane/polyaniline composite properties: The enhancement of electrical and mechanical properties for medical tissue engineering. *AIMS Mater Sci* 11: 323–342. <https://doi.org/10.3934/matersci.2024018>
2. Ananthan VB, Bernicke P, Akkermans RA, et al. (2020) Effect of porous material on trailing edge sound sources of a lifting airfoil by zonal overset-LES. *J Sound Vib* 480: 115386. <https://doi.org/10.1016/j.jsv.2020.115386>

3. Geyer T, Sarradj E, Fritzsche C (2010) Measurement of the noise generation at the trailing edge of porous airfoils. *Exp fluids* 48: 291–308. <https://doi.org/10.1007/s00348-009-0739-x>
4. Shen Y, Jiang G (2016) The influence of production parameters on sound absorption of activated carbon fiber felts. *J Text I* 107: 1144–1149. <https://doi.org/10.13475/j.fzxb.20191205805>
5. Das P, Manna S, Behera AK, et al. (2022) Current synthesis and characterization techniques for clay-based polymer nano-composites and its biomedical applications: A review. *Environ Res* 212: 113534. <https://doi.org/10.1016/j.envres.2022.113534>
6. Dong Y, Bhattacharyya D (2012) Investigation on the competing effects of clay dispersion and matrix plasticisation for polypropylene/clay nanocomposites. Part II: Crystalline structure and thermo-mechanical behaviour. *J Mater Sci* 47: 4127–4137. <http://doi.org/10.1007/s10853-012-6248-y>
7. Mohammed L, Biglari H, Vakili-Tahami F (2023) Analyzing the buckling of FGCNT-reinforced sandwich microshells in heart pacemakers: The impact of thickness stretching on third-order shear deformation. *AIP Adv* 13: 075026. <https://doi.org/10.1063/5.0157650>
8. Lee PC, Kang D, Oh JT, et al. (2023) Reducing moisture absorption in polypropylene nanocomposites for automotive headlamps using hydrophobicity-modified graphene/montmorillonite. *Nanomaterials-Basel* 13: 1439. <https://doi.org/10.3390/nano13091439>
9. Wang J, Pei S, Yang Y, et al. (2024) Convolutional transformer-driven robust electrocardiogram signal denoising framework with adaptive parametric ReLU. *Math Biosci Eng* 21: 4286–4308. <https://doi.org/10.3934/mbe.2024189>
10. Zhong W, Mao L, Du W (2023) A signal quality assessment method for fetal QRS complexes detection. *Math Biosci Eng* 20: 7943–7956. <https://doi.org/10.3934/mbe.2023344>
11. Wen P, Zhang Y, Wen G (2023) Intelligent personalized diagnosis modeling in advanced medical system for Parkinson’s disease using voice signals. *Math Biosci Eng* 20: 8085–8102. <https://doi.org/10.3934/mbe.2023351>
12. Justice DH, Trussell HJ, Olufsen MS (2006) Analysis of blood flow velocity and pressure signals using the multipulse method. *Math Biosci Eng* 3: 419–440. <https://doi.org/10.3934/mbe.2006.3.419>
13. Saurav S, Mohan A, Tabassum Z, et al. (2024) Recent trends in polymer-based nanocomposites and its application in bone tissue engineering. *AIP Conference Proceedings AIP Publishing* 2986: 030138. <https://doi.org/10.1063/5.0197881>
14. Sagadevan S, Schirhagl R, Rahman MZ, et al. (2023) Recent advancements in polymer matrix nanocomposites for bone tissue engineering applications. *J Drug Deliv Sci Tec* 82: 104313. <https://doi.org/10.1016/j.jddst.2023.104313>
15. Abbas M, Alqahtani MS, Alhifzi R (2023) Recent developments in polymer nanocomposites for bone regeneration. *Int J Mol Sci* 24: 3312. <https://doi.org/10.3390/ijms24043312>
16. Cingolani E, Goldhaber JJ, Marbán E (2018) Next-generation pacemakers: From small devices to biological pacemakers. *Nat Rev Cardiol* 15: 139–150. <https://doi.org/10.1038/nrcardio.2017.165>
17. Nordi TM, Gounella RH, Ginja GA, et al. (2023) Low-noise amplifier and neurostimulator in submicron CMOS for closed-loop deep-brain stimulation (CLDBS). *Preprints* 5: 1182. <https://doi.org/10.20944/preprints202305.1182.v1>

18. Uppu V, Mishra K, Babu LK, et al. (2019) Understanding the influence of graphene and nonclay on the microcracks developed at cryogenic temperature. *AIMS Mater Sci* 6: 559–566. <https://doi.org/10.3934/matersci.2019.4.559>
19. Safie NE, Azam MA (2022) Understanding the structural properties of feasible chemically reduced graphene. *AIMS Mater Sci* 9: 617–627. <https://doi.org/10.3934/matersci.2022037>
20. Di-Gianni A, Amerio E, Monticelli O, et al. (2008) Preparation of polymer/clay mineral nanocomposites via dispersion of silylated montmorillonite in a UV curable epoxy matrix. *Appl Clay Sci* 42: 116–124. <https://doi.org/10.1016/j.clay.2007.12.011>
21. Wang H, Feng Q, Liu K (2016) The dissolution behavior and mechanism of kaolinite in alkali-acid leaching process. *Appl Clay Sci* 132: 273–280. <https://doi.org/10.1016/j.clay.2016.06.013>
22. Zaaba NI, Foo KL, Hashim U, et al. (2017) Synthesis of graphene oxide using modified hummers method: Solvent influence. *Procedia Eng* 184: 469–477. <https://doi.org/10.1016/j.proeng.2017.04.118>
23. Kumar V, Singh A (2013) Polypropylene clay nanocomposites. *Rev Chem Eng* 29: 439–448. <https://doi.org/10.1515/revce-2013-0014>
24. Patra SC, Swain S, Senapati P, et al. (2022) Polypropylene and graphene nanocomposites: Effects of selected 2D-nanofiller's plate sizes on fundamental physicochemical properties. *Inventions* 8: 8. <https://doi.org/10.3390/inventions8010008>
25. Lin C, Wen G, Yin H, et al. (2022) Revealing the sound insulation capacities of TPMS sandwich panels. *J Sound Vib* 540: 117303. <https://doi.org/10.1016/j.jsv.2022.117303>
26. Rastegar S, Stadlbauer J, Pandhi T, et al. (2019) Measurement of signal-to-noise ratio in graphene-based passive microelectrode arrays. *Electroanaly* 31: 991–1001. <https://doi.org/10.1002/elan.201800745>
27. Li F, Wang R, Zheng Z, et al. (2022) A time-variant reliability analysis framework for selective laser melting fabricated lattice structures with probability and convex hybrid models. *Virtual Phys Prototy* 17: 841–853. <https://doi.org/10.1080/17452759.2022.2074196>
28. Naffakh M, Fernández M, Shuttleworth PS, et al. (2020) Nanocomposite materials with poly (l-lactic acid) and transition-metal dichalcogenide nanosheets 2D-TMDCs WS<sub>2</sub>. *Polymers-Basel* 12: 2699. <https://doi.org/10.3390/polym12112699>
29. Liu J, Chen T, Zhang Y, et al. (2019) On sound insulation of pyramidal lattice sandwich structure. *Compos Struct* 208: 385–394. <https://doi.org/10.1016/j.compstruct.2018.10.013>
30. Glé P, Gourdon E, Arnaud L (2011) Acoustical properties of materials made of vegetable particles with several scales of porosity. *Appl Acoust* 72: 249–259. <http://dx.doi.org/10.1016/j.apacoust.2010.11.003>
31. Othmani C, Taktak M, Zain A, et al. (2017) Acoustic characterization of a porous absorber based on recycled sugarcane wastes. *Appl Acoust* 120: 90–97. <https://doi.org/10.1016/j.apacoust.2017.01.010>
32. Pan G, Zhao Y, Xu H, et al. (2016) Acoustical and mechanical properties of thermoplastic composites from discarded carpets. *Compos Part B-Eng* 99: 98–105. <https://doi.org/10.1016/j.compositesb.2016.06.018>
33. Martinez L, Palessonga D, Roquefort P, et al. (2021) Development of a high temperature printable composite for microwave absorption applications. *AIMS Mater Sci* 8: 739–747. <https://doi.org/10.3934/matersci.2021044>

34. Rafiee M, Abidnejad R, Ranta A, et al. (2021) Exploring the possibilities of FDM filaments comprising natural fiber-reinforced biocomposites for additive manufacturing. *AIMS Mater Sci* 8: 524–537. <https://doi.org/10.3934/matersci.2021032>
35. Satour A, Montrésor S, Bentahar M, et al. (2014) Acoustic emission signal denoising to improve damage analysis in glass fibre-reinforced composites. *Nondestruct Test Eva* 29: 65–79. <https://doi.org/10.1080/10589759.2013.854782>
36. Harrouche K, Rouvaen JM, Ouafitouh M, et al. (2000) Signal-processing methods for analysing the structure of carbon-epoxy-resin composite materials. *Meas Sci Technol* 11: 285. <https://iopscience.iop.org/article/10.1088/0957-0233/11/3/317/meta>
37. Li Z, Xiang S, Lin Z, et al. (2021) Graphene oxide-functionalized nanocomposites promote osteogenesis of human mesenchymal stem cells via enhancement of BMP-SMAD1/5 signaling pathway. *Biomaterials* 277: 121082. <https://doi.org/10.1016/j.biomaterials.2021.121082>
38. Aydın G, San SE (2024) Breaking the limits of acoustic science: A review of acoustic metamaterials. *Mat Sci Eng B-Adv* 305: 117384. <https://doi.org/10.1016/j.mseb.2024.117384>
39. Yang X, Wen G, Jian L, et al. (2024) Archimedean spiral channel-based acoustic metasurfaces suppressing wide-band low-frequency noise at a deep subwavelength. *Mater Design* 238: 112703. <https://doi.org/10.1016/j.matdes.2024.112703>
40. Wen G, Zhang S, Wang H, et al. (2023) Origami-based acoustic metamaterial for tunable and broadband sound attenuation. *Int J Mech Sci* 239: 107872. <https://doi.org/10.1016/j.ijmecsci.2022.107872>
41. Suherman H (2019) Optimization of compression moulding parameters of multiwall carbon nanotube/synthetic graphite/epoxy nanocomposites with respect to electrical conductivity. *AIMS Mater Sci* 6: 621–634. <https://doi.org/10.3934/matersci.2019.4.621>
42. Kiddell S, Kazemi Y, Sorken J, et al. (2023) Influence of flash graphene on the acoustic, thermal, and mechanical performance of flexible polyurethane foam. *Polym Test* 119: 107919. <https://doi.org/10.1016/j.polymertesting.2022.107919>
43. Suhr J, Koratkar N, Koblinski P, et al. (2005) Viscoelasticity in carbon nanotube composites. *Nat mater* 4: 134–137. <https://doi.org/10.1038/nmat1293>
44. Rahbarshendi F, Baybordiani A, Asgharzadeh H, et al. (2022) The effect of graphene-based nanofillers on the structure, thermal, and mechanical properties of poly (vinyl alcohol). *J Appl Polym Sci* 139: e52664. <https://doi.org/10.1002/app.52664>
45. Charandabinezhad SR, Asgharzadeh H, Arsalani N (2021) Synthesis and characterization of reduced graphene oxide/magnetite/polyaniline composites as electrode materials for supercapacitors. *J Mater Sci-Mater El* 32: 1864–1876. <https://doi.org/10.1007/s10854-020-04955-7>
46. Asgharzadeh H, Eslami S (2019) Effect of reduced graphene oxide nanoplatelets content on the mechanical and electrical properties of copper matrix composite. *J Alloy Compd* 806: 553–565. <https://doi.org/10.1016/j.jallcom.2019.07.183>
47. Jafarlou H, Hassannezhad K, Asgharzadeh H, et al. (2018) Enhancement of mechanical properties of low carbon steel joints via graphene addition. *Mater Sci Tech-lond* 34: 455–467. <https://doi.org/10.1080/02670836.2017.1407543>
48. Abdolhosseinzadeh S, Asgharzadeh H, Seop Kim H (2015) Fast and fully-scalable synthesis of reduced graphene oxide. *Sci Rep* 5: 10160. <https://doi.org/10.1038/srep10160>



49. Khameneh-Asl S, Namdar-Habashi M, Kianvash A, et al. (2019) Fabrication of graphene/MoS<sub>2</sub> nanocomposite for flexible energy storage. *J Nanostruct* 9: 21–28. <https://www.sid.ir/paper/750795/en>
50. Asl SK, Namdar M (2019) Preparation of graphene/graphene oxide microsupercapacitor by using laser-scribed method. *Chem Methodol* 3: 183–193. <https://doi.org/10.22034/chemm.2018.144016.1073>
51. Schaldach M (1992) Materials in pacemaker technology, *Electrotherapy of the Heart: Technical Aspects in Cardiac Pacing*, Berlin: Springer, 169–190. <https://doi.org/10.1007/978-3-642-50209-5>
52. Upadhyay S, Upadhya A, Salehi W, et al. (2021) The medical aspects of EMI effect on patients implanted with pacemakers. *Mater Today Proceed* 45: 5243–5248. <https://doi.org/10.1016/j.matpr.2021.01.826>
53. Cai Y, Hang Y, Zhou Y, et al. (2019) Graphene-based biosensors for detection of composite vibrational fingerprints in the Mid-infrared region. *Nanomaterials-Basel* 9: 1496. <https://doi.org/10.3390/nano9101496>



AIMS Press

© 2024 the Author(s), licensee AIMS Press. This is an open access article distributed under the terms of the Creative Commons Attribution License (<https://creativecommons.org/licenses/by/4.0>)